

RIGA TECHNICAL UNIVERSITY

Dmitrijs MERKULOVŠ

**CYLINDRICAL CELL BASED REFRACTOMETER AND ITS
APPLICATIONS METHODOLOGY**

Field: Mechanical engineering
Subfield: Measurements instrumentation and metrology

Dr. sc. eng. Thesis summary

Riga 2015

RIGA TECHNICAL UNIVERSITY
Faculty of Transport and Mechanical Engineering
Biomedical engineering and nanotechnology institute

Dmitrijs MERKULOV

Doctoral student of the Dr. sc. eng. study program "Engineering Technology, Mechanics and Mechanical Engineering (RMDM8)"
The direction "Medical engineering and medical physics"

**CYLINDRICAL CELL BASED REFRACTOMETER AND ITS
APPLICATIONS METHODOLOGY**

Field: Mechanical engineering
Subfield: Measurements instrumentation and metrology

Dr. sc. eng. Thesis summary

Supervisors
Dr. habil. phys.
Y. DEKHTYAR
Dr. habil. sc. eng.
P. SHIPKOV

Riga 2015

UDK 543.452
MD 7S

Merkulovs D. Cylindrical
cell based refractometer and
its applications methodology
Dr. sc. eng. thesis summary
R.: RTU, 2015- 32 p.

It has been printed according
to the order of RTU TME BENI
From 22nd of January 2015.
The protocol
No 3.



European Social Fund



European Union

This work has been supported by the European Social Fund within the project
"Support for the implementation of doctoral studies at the Riga Technical University"
#2009/0144/1DP/1.1.2.1.2/09/IPIA/VIAA/005

**THIS DOCTORAL THESIS HAS SUBMITTED FOR THE AWARD OF A
DEGREE OF DOCTOR OF ENGINEERING SCIENCES AT RIGA
TECHNICAL UNIVERSITY**

Promotion work for obtaining engineering sciences doctoral scientific degree will be defended in 30th of June 2015 (3 pm) in the Riga Technical University, faculty of Transport and Engineering Science, address: 6 Ezermalas street, room 405.

OFFICIAL OPPONENTS

Juris Krizbergs, Dr. sc. ing.
Riga Technical University

Viktors Gavrilovs, Dr. Phys.
Institute of Physical Energetic, Latvian Academy of Sciences

Yuri Nikitenko, Dr. Phys.
Joint Institute for Nuclear Research (JINR), Dubna, Russia

CONFIRMATION

I confirm that I have developed this thesis, submitted to the Riga Technical University to obtain the engineering doctoral degree. This thesis has not been submitted to any other university to get the degree.

Dmitrijs Merkulovs.....(Signature)

Date:

The thesis is written in English. It contains of an introduction, 4 chapters and resume. It is written on 118 pages, contains 52 figures, 9 tables, 116 references and 10 appendixes.

CONTENTS

GENERAL DESCRIPTION OF THE DOCTORAL THESIS	5
Actuality of the theme	5
Goal and task of the research	5
Research methods	5
Scientific novelty	6
Practical applicability	6
Theses to defend	6
The list of the main publications	6
Content and structure of the doctoral thesis	8
DESCRIPTION OF THE THESIS	9
Exploration of the terms and abbreviations used in this work	9
Chapter 1. REFRACTION INDEX AND CONTENTS OF LIQUIDS	9
1.1. Refractive index measurement principle	9
1.2. Concentration of the components of the liquids, its density and refractive index	10
1.3. The influence of temperature of liquids on the refractive index	12
1.4. Refractive index in dependence on the wavelength	12
Chapter 2. REFRACTOMETERS. STATE OF THE ART	13
Chapter 3. MULTIPLE LIGHT BEAM REFRACTION AND REFLECTION IN THE CYLINDRICAL CELL WITH THE TEST SOLUTION	13
3.1. The physical approach of the cylindrical cell based refractometers	13
3.2. Influence of the refractive index on the light deviation in the exit of the refractometer	14
3.3. Cylindrical cell based refractometers and fundamentals of the theory	16
3.4. Mathematical simulation of the refractometers	21
3.5. Approach to analyse the image by cylindrical cell based refractometer	22
Chapter 4. CYLINDRICAL CELL BASED REFRACTOMETERS FOR MEASUREMENTS OF REFRACTIVE INDEXES OF LIQUIDS	23
4.1. Scheme of the refractometers	24
4.2. Algorithm of processing of measurements results	25
4.3. The calibration of the refractometers	26
4.4. Approach to properties of the refractometers	29
CONCLUSION	31
REFERENCES	32

GENERAL DESCRIPTION OF THE DOCTORAL THESIS

Actuality of the theme

The refractive index (RI) of a liquid carries important information about its physical properties, including concentration and density, thus making it possible to determine and monitor the composition of the solution.

Purpose of the thesis was to create a refractometer and methodology to reach a higher as compared to present devices resolution of RI measurements. For this purpose the RI is measured as the deviation of a laser beam passed several times through a cylindrical cell containing the tested liquid.

To provide RI detection of liquids, various types of measurement methods and measuring devices [2, 3, 5, 6, 8, 9, 11, 17, 19] are conventionally used, in dependence on the measured object diversity and specificity of the measurement tasks and measurement resolution required.

Currently available compact portable refractometers do not provide the RI measurement with a resolution over 10^{-4} of the RI.

There is an increasing demand for a compact and inexpensive RI measuring devices that provide the resolution of 10^{-5} and higher.

The magnitude of the deviation, which depends on the RI, is measured as the displacement of the transmitted beam's projection on a linear measuring element, such as a linear CMOS or CCD image sensor. In order to significantly improve the resolution of RI measurements, an efficient solution has been developed, based on repeated reflection and refraction of the light beam travelling through the cylindrical cell with liquid. A new method for detecting the position of the projected laser beam on a linear optical sensor was developed, too.

The new refractometer provides more than ten times higher measurement resolution as compared to the existing instruments, and has more than ten times smaller sizes and weight, and does not depend on the stability of the structural elements of the device.

Goals and tasks of the research

The goals:

To develop a new physical fundamentals and approach to create and use a portable refractometer with high RI resolution ($\sim 10^{-5}$).

The tasks:

1. To develop the physical fundamentals of the cylindrical cell based refractometer (CCR).
2. To develop the mathematical model of CCR to determine the properties of the refractometers.
3. To develop the CCR prototype, including optical, electronic, computing and mechanical systems.
4. To develop the CCR calibrate methodology, its algorithm for measurements of the RI and concentrations of the solutions.
5. To explore RI measurement resolution available from the CCR.
6. To verify of CCR practical applicability.

Research methods

In order to achieve the objectives of this work and realize the given tasks, the following research methods have been used during the development of the dissertation:

Origin 6.1 – mathematical statistics (regression analysis);

Mathcad 14 - mathematical modelling and measurement data processing.

Tables, charts and images are used to ensure the obviousness of the research results.

Scientific novelty

For the first time:

1. The basic operating principles of the refractometers were developed, where an optical beam refraction and multiple reflections in a cylindrical cell has been used, in such a way increasing the RI measurement resolution by one power and achieving $MR = 10^{-5}$.
2. The mathematical model has been developed and analyzed, which takes into account the temperature effect on the detection of resolution, the possibility to achieve the resolution up to 10^{-7} has been demonstrated. It has been shown; that the multiple light beam passage through cylindrical cell with test liquid increases the RI measurement resolution in line with the number of the passage cycles.
3. The RI measurement algorithm and measurement method have been developed, where a minimum place of the detectable beam interference pattern has been used, that allows to achieve the RI measurement resolution $2 \cdot 10^{-5}$.

Practical application implementation

- CCR with a new physical principle of RI measurement and concentrations of the solution has been used in the following projects:
 - Project "Methanol fuel cell sensor adaptation and other control and measurement systems" TOP 06-14. Institute of Physical Energetic, Riga, Latvia.
 - ERAF project "Innovative bio-ethanol dehydration technology and design parameters of the measuring device" 010/0281/2DP/2.1.1.1.0/10/APIA/VIAA/003. Institute of Physical Energetic, Riga, Latvia.
- Company ELMI Ltd (Riga, Latvia) has commenced the manufacturing process of 6 CCR prototypes for commercial use and market research. These prototypes were demonstrated at the Pittsburg Conference (Pittcon) in Chicago, IL, USA on July 27 2014. Currently these devices operate in the United States and Germany.

Theses to defend

1. The new refractometer has been designed and developed. It is equipped with the original optical and control system, and these systems allow many times to increase the MR.
2. The mathematical model of the new CCR is created, that confirms the possibility of increasing the resolution of the RI measurement by 3 powers as compared with the conventional refractometers (from 10^{-4} to 10^{-7}).
3. The new RI measurement algorithm has been developed. This algorithm employs the detectable beam interference pattern of the first minimum space, in such a way increasing the RI measurement resolution (MR) up to 10^{-5} .
4. The new CCR provides the improved resolution (by one power) of the concentration measurements of the calibrated solutions (sugar, sodium chloride, ethanol-water solutions).
5. The new CCR has been created and calibrated, and the testing process of this device has been provided.

The list of the main publications

- Papers

1. Kozlov V., Merkulov D., Vilitis O., New method for measuring refractive index of liquids Proc. SPIE 4318, Smart Optical Inorganic Structures and Devices, 89 (March 8, 2001),pp. 89-92. ISSN: 0091-3286, e-ISSN: 1560-2303 doi:10.1117/12.417582. (SCOPUS bibliographic database).
2. Vilitis O., Merkulovs D., Optical cell for measuring refractive index and concentration of liquids, Latvian Journal of Physics and Technical Sciences, Riga, 2004, 4 p.58–66. ISSN 0868 - 8257.

3. Vilitis O., Šipkovs P., Merkulovs D., Refrakcijas indeksa noteikšana šķidrumiem cilindriskā ķivetē, *Latvian Journal of Physics and Technical Sciences*, Riga, 2008, vol.45, no. , pp.50–62. ISSN 0868-8257.
4. Vilitis O., Shipkovs P., Merkulovs D., Determining the liquids refractive index by using a cylindrical cuvette, *Measurements science and technology*, 2009, no. 20, 117001 (8pp), ISSN 1361-6501, eISSN 1361-6501, doi:10.1088/0957-0233/20/11/117001. (SCOPUS bibliographic database).
5. Vilitis O., Shipkovs P., Merkulovs D., Determination of two-liquid mixture composition by assessing dielectric parameters 1. Precise measuring system, *Latvian Journal of Physics and Technical Sciences*, Riga, 2013, no.4, pp.62–73. ISSN 0868 - 8257. DOI: 10.2478/ipts-2013-0027. (SCOPUS bibliographic database).
6. Vilitis O., Shipkovs P., Merkulovs D., Rucins A., Zihmane-Ritina K., Bremers G. Determination of two-liquid mixture composition by assessing its dielectric parameters 2. Modified measuring system for monitoring the dehydration process of bioethanol production, *Latvian Journal of Physics and Technical Sciences*, Riga, 2014, no.1, pp.54–61. ISSN 0868 - 8257. DOI: 10.2478/ipts-2014-0006. (SCOPUS bibliographic database).
7. Merkulovs D., Dekhtyar Y., Vilitis O., Shipkovs P., Merkulova V., *Cylindrical Cuvette Light Refraction Measurements Technology to Analyses Biomedical Liquids*, International Federation for Medical and Biological Engineering (IFMBE), Volume 45, 2015, pp 298-301, DOI:10.1007/978-3-319-11128-5_74, Online ISBN:978-3-319-11128-5, ISSN:1680-0737 (Springerlink).

- Patents

1. Vilitis O., Kozlovs V., Merkulovs D., Mironovs I., Divstaru refraktometers, Patents LV12549, International Publication Date 20.12.2000.
2. Vilitis O., Kozlovs V., Merkulovs D., Plaša diapazona šķidrumu laušanas koeficienta mērīšanas paņēmiens un refraktometers tā īstenošanai, Patents LV13294, International Publication Date 20.05.2005.
3. Vilitis O., Merkulovs D., Refraktometra gaismas staru kūļa optiskā attēla detektēšanas paņēmiens, Patents LV13598, International Publication Date 20.09.2007.
4. Vilitis O., Šipkovs P., Merkulovs D., Šķīdumu koncentrācijas mērīšanas paņēmiens un sensors tā īstenošanai, Patents LV13728, International Publication Date 20.07.2008.

- Conference abstracts

1. Merkulovs D., Kozlovs V., Vilitis O. A new methods for measuring refractive index of liquids, 2-nd International Conference «Advanced Optical Materials and Devices», Vilnius, 16-19 August, 2000, Semiconductor Physics Institute, Lithuania 2000 lpp 33, ISSN 1392-0952.
2. Merkulovs D., Vilitis O., Kozlovs V. Refractometer DBR-11, New Method for Measuring Refractive Index of Transparent liquids, Hightechbaltic2001, Exhibition Research Technologies Innovation 2001, International Exhibition Centre, Riga, September 14-15.
3. Merkulovs D., Vilitis O., Kozlovs V. Refractometer, 23-th Inter-national Award for Technology and Quality. New Millenium Award, (Trade Leader's Club), December 21, 2001, Madrid, Spain; January 10-12, 2002, Geneva, Switzerland.
4. Merkulovs D., Vilitis O., Kozlovs V. Double beam detector of refractive index – main features, 3rd International Conference on Advanced Optical Materials and Devices AOMD-3, Riga, August 19-22, 2002.
5. Merkulovs D., Vilitis O., Kozlovs V. Pocket Refractometer, Baltic Industry 2003, November 5-8, 2003.

6. Merkulovs D., Vilitis O., Shipkovs P. Determining the liquids refractive index by using a cylindrical cuvette, 54th International Scientific Conference, Riga, Latvia, October 14-16, 2013.
7. Merkulovs D., Vilitis O., Shipkovs P. Determination of two-liquids mixture composition by assessing dielectric parameters, 54th International Scientific Conference, Riga, Latvia, October 14-16, 2013.
8. Merkulovs D., Dekhtyar Y., Vilitis O., Shipkovs P. and Merkulova V. Cylindrical cuvette light refraction measurements technology to analyze biomedical liquids, Medical and Biological Engineering (MBEC 2014), Dubrovnik, Croatia 7.-11. sept., 2014.
9. Merkulovs D., Dekhtyar Y., Vilitis O., Shipkovs P. and Merkulova V. Precision cylindrical cell's refractometer to analyze biomedical liquids, 55th International Scientific Conference, Riga, Latvia, October 16-18, 2014.

The main results were presents at 9 conferences (3 international, 6 in Latvia).

- Exhibitions and seminars

1. Refractometers were demonstrated at the exhibition BIOTECHNICA 2013, 08.10.2013-10.10.2013 in Hanover, Germany.
2. Seminar in RTU Biomedical Engineering and Nanotechnology Institute 22.01.2015, Riga, Latvia.
3. Seminar in Latvian National Mechanics Committee (LNMK) and RTU Institute of Mechanics (MI) 17.02.2015, Riga, Latvia.

Content and structure of the doctoral thesis

The thesis is written in English. It contains of an introduction, 4 chapters and resume. It is written on 118 pages, contains 52 figures, 9 tables, 116 references and 10 appendixes.

DESCRIPTION OF THE THESIS

Exploration of the terms and abbreviations used in this work

<i>a</i>	optical element cylinder axis distance range exceeded the mid-point of the linear scale measuring element;
<i>c</i>	speed of light in vacuum;
<i>C</i>	concentration;
<i>d</i>	density;
<i>k</i>	optical element cylinder radius ratio r_1/r_2 ;
<i>L</i>	cylinder axis of the optical element of the linear distance measured in the plane of the element and the optical input-output center edge angle of intersection of the beginning
<i>m</i>	optical element beam output sequence number;
<i>M</i>	mass, kg;
<i>n</i>	refractive index;
<i>n₁</i>	ambient refractive index;
<i>n₂</i>	optical element material cell refractive index;
<i>n₃</i>	the liquid refractive index;
<i>r₁</i>	optical element cylinder outer radius;
<i>r₂</i>	an optical element inside radius of the cylinder;
<i>t</i>	the temperature;
<i>Q</i>	optical element beam exit point;
<i>α</i>	angles;
<i>β</i>	angles;
<i>v</i>	the velocity of light in the respective medium
<i>η</i>	an optical element in the optical input-output center angle;
<i>λ</i>	the wavelength of that light;
<i>Ψ</i>	an optical element in the optical input-output center angle of the start edge angle relative to the plane of the linear measuring element;
ADC	analog-to-digital converter;
CCD	charge-coupled device;
CCR	the cylindrical cell based refractometer;
CMOS	complementary metal-oxide semiconductor;
MCU	microprocessor control unit;
MR	the RI measurement resolution;
RI	the refractive index.

Chapter 1. REFRACTION INDEX AND CONTENTS OF LIQUIDS

1.1. Refractive index measurement principle

This chapter is devoted to review of the literature about physical principles of refractometers measuring the refractive index of light in liquids.

Refractive index (RI) is an important characteristic of liquid substances for analyzing, monitoring, and identification of liquid substances in several industries nowadays. Accurate determination of the concentration of the solution by measuring the RI is widely used in chemical and physical studies, food technology, materials processing, medical diagnostics, monitoring systems, fuel cells directly measuring pollution, and many other fields.

Refractive index (RI) relates to of the speed of light in a medium. The refractive index (n) of a medium is defined as the ratio of speed of light in vacuum ($c=299\ 792\ 458$ m/s) in to that in the medium (v):

$$n = \frac{c}{v} \quad (1.1)$$

As the speed of light is highest in vacuum $c > v$, n is always greater than 1.

Snell's law states that the ratio of the sines of the angles of incidence and refraction is equivalent to the ratio of phase velocities of light in the two media, or equivalent to the reciprocal of the ratio of the indices of refraction:

$$\frac{\sin \alpha_1}{\sin \beta_1} = \frac{v_1}{v_2} = \frac{n_2}{n_1}, \quad (1.2)$$

with each α_1 , β_1 as the angle measured from the normal of the boundary, v as the velocity of light in the respective medium (SI units are meters per second, or m/s) and n as the refractive index (which is unitless) of the respective medium [16].

The speed of light in medium depends on the temperature and wavelength. Due to the wavelength dependence on the speed of light, the refractive index is measured with monochromatic light. The common practice is to use the yellow sodium D-line wavelength 589.3 nm. The refractive index measured at this wavelength is usually denoted by n_D . The standard temperature is +20°C or +25°C [18].

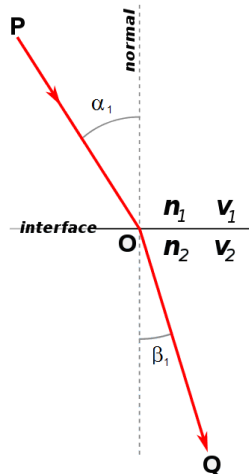


Fig. 1.1. Refraction of light at the interface between two medias of different refractive indices

1.2. Concentration of the components of the liquids, its density and refractive index

In general, the measured refractive index of a multicomponent mixture is a function of its temperature T , concentration C , and the wavelength of the incident light λ [5]:

$$n = n(T, C, \lambda) \quad (1.3)$$

In sections 1.3 and 1.4 the dependence of temperature and wavelength of light on RI will be considered in detail.

From Eq.(1.3)., the change of RI Δn of a multicomponent mixture is:

$$\Delta n \approx \frac{\partial n}{\partial T} \Delta T + \frac{\partial n}{\partial C} \Delta C + \frac{\partial n}{\partial \lambda} \Delta \lambda, \quad (1.4)$$

for small changes of the temperature, concentration, and wavelength. Since laser light is highly monochromatic and wavelength-stable, $\Delta\lambda \approx 0$ and wave length effects can be neglected. In this work, the concentration is de fined on a mass basis for liquids A and B,

$$C_A = \frac{M_A}{M_A + M_B}, \quad (1.5)$$

$$C_B = \frac{M_B}{M_A + M_B}, \quad (1.6)$$

were M - mass, kg.

Usually RI increases with increasing density. Theoretical study of the relationship between the density of matter and its RI, as well as the experimental data shows that there is a direct proportion between some RI function $f(n)$ and density d :

$$f(n) = rd \quad (1.7)$$

The constant factor r that is specific for this substance is called as specific refraction.

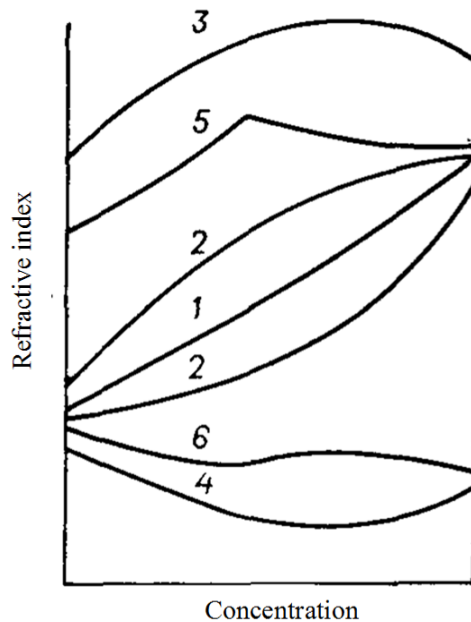


Fig. 1.2. Types of curves characterizing refractive index - concentration (composition):
1 - with a small curvature; 2 - with a big curvature; 3 - with the maximum; 4 - with a minimum; 5 - with the singular point; 6 - to the point of inflection [18]

The concentration can be calculated from the refractive index and temperature when these nonlinear functions are known. There are several possible temperature compensation algorithms. In practical use, a simple 3rd degree polynomial is typically used.

By applying data analysis program the experimental data were subjected to curve fitting and the temperature coefficient of refractive index of water was found to be equal to $-1.853 \times 10^{-4} \text{C}^\circ$. For measurements with high resolution, the optical constants of the glass container should also be taken in account because the light will pass through both the solution and the container. According to the literature [18], the temperature coefficient of refractive index of glass is of the order of 10^{-4}C° . It is evident that very small error can occur if the temperature dependence of the refractive index of glass is not taken into account while measuring the temperature coefficient of refractive index of liquids.

1.3. The influence of temperature of liquids on the refractive index

The first created refractometers in the world were not equipped with any temperature compensation. Therefore, they almost did not find any wide application in practice. And only then, when it was possible to manufacture refractometers with thermal stabilization, and it happened in the late 19th century, refractometers have been widely used in practice [16, 18].

The influence of temperature and pressure on the RI is determined by the following two factors:

- 1) changing the number of particles per unit of volume when we have heating or pressure (i.e., expansion coefficient and compressibility coefficient), and
- 2) dependence on the polarizability of the molecules according to the temperature and pressure.

A linear extrapolation of the variables n is permissible for some small temperature difference (10-20°C). Already in the temperature range of 40-60°C for organic liquids a clearly expressed (and not strictly linear) dependence $\partial n / \partial t$ on the temperature is found. Accurate calculations n for a wide temperature range are made from the empirical formulas as follows:

$$n_t = n + a \cdot t + b \cdot t^2 \dots, \quad (1.8)$$

where a , b - coefficients.

As an example we can use the empirical formula expressing the temperature dependence of the benzol RI up to the boiling point:

$$n_t = 1.51431 - 6.44 \cdot 10^{-4} t + 0.033 \cdot 10^{-6} t^2 - 2.391 \cdot 10^{-9} t^3 \quad (1.9)$$

In liquids and solids, the compressibility is very small; the increase in pressure of 1 atm is generally increasing n by several units of 10^{-5} .

It is shown that there is not any linear relationship between the RI and all of these mentioned factors [18].

High sensitivity of the RI measurements in aqueous solutions depending on concentrations and density makes these refractometers as highly sensitive devices. However, a great influence of the temperature on the resolution of the RI measurements requires taking into account the temperature change already from 10^{-4} RI [18].

1.4. Refractive index in dependence on the wavelength

The refractive index can be seen as the factor by which the speed and the wavelength of the radiation are reduced with respect to their vacuum values: the speed of light in a medium is Eq.(1.1), and similarly the wavelength in that medium is:

$$\lambda = \frac{\lambda_0}{n}, \quad (1.10)$$

where λ_0 is the wavelength of that light in vacuum.

The refractive index varies with the wavelength of light.

In the reference literature for the media materials the data n are mainly referred. These data correspond to the standard wavelength. In these developed refractometers a laser with a non-standard wavelength is employed and for mathematical calculations empirically obtained approximation formulas are used. The resolution of the RI measurements obtained in this manner can reach to 10^{-5} . There is an extensive database of RI depending on the wavelength of the laser [7].

Chapter 2. REFRACTOMETERS. STATE OF THE ART

This chapter includes an overview of the basic structures of classical refractometers (Abbe refractometer, Pulfrich refractometer), including a special class of cell based refractometers used as a measuring element of the wall of the cell with the test solution.

Despite the fact that the refractometry research methods are used already a very long period of time, all the time there are new publications describing some innovative approaches in refractometry, because the old classical refractometers are not available to cope with the growing demands of modern technologies. Therefore, there is a demand of constant search for new design ideas and technologies in a refractometry.

In the modern world, there is a great need for precision refractometers with small dimensions and weight, because sensors very often must be build into a variety of technological systems for chemical and biological industries, where placement of sensors with large dimensions and weight is a big problem. Refractometers made by the classical scheme can not always be used here.

For medical practices, it is necessary to have more and more accurate refractometers to provide a remote analysis of the patients' conditions. In addition to the traditional use of refractometry as a method of analyzing the content of sugar in the blood and urine of patients, serological blood tests, determination of protein in urine, measurement the density of urine, analysis of the brain fluid, density determination of the intraocular liquid, etc, constantly there are new ways of the possible use of the refractometer, requiring simpler operating principles and more suitable construction for mass production.

Additionally there is a great need for small sensors for quality control in the bio-fuel industry.

Portable and precise refractometers are necessary to ensure the safety and protection of the environment and for use in household.

Very important is the price of a refractometer and a power consumption of this device.

CCR have a special place in the field of refractometry. They play a unique role in the control of a real-time fundamental research, in chemical analysis and medical diagnostics, as well as in the processing and manufacturing of various substances. Opportunity to get maximally close to the test solution, simple design of the refractometer, ability to easily solve the problem of creating a flow measuring cells makes them beyond the competition with well-known classical refractometers.

Considered the design and specifications of modern refractometers in this chapter and the advantages and disadvantages of the known refractometers are discussed.

The first and the second chapters included the information about goals and tasks of the research.

Chapter 3. MULTIPLE LIGHT BEAM REFRACTION AND REFLECTION IN THE CYLINDRICAL CELL WITH THE TEST SOLUTION

This chapter is devoted:

- to the development and investigation of the physical fundamentals of the cylindrical CCR,
- to the research and development of the mathematical model of CCR to determine the properties of the refractometers.

3.1. The physical approach of the cylindrical cell based refractometers

One of the ways to increase the sensitivity of the refractometer can be multiple passage of the light beam through the sample when the light beam passes each time through the following

system: [wall] - [the sample for investigation] - [wall] - [the sample for investigation] - and so on. It greatly increases the exiting angle of the beam at the end from the cell.

The more are these reflections; the bigger is the angle of the outgoing light beam, going from the cylindrical cell. Below it will be shown **that the deflection angle of the light beam coming from the cylindrical cell increases as many times as the number of reflections of the beam inside the cell.**

All classical type Abbe or Pulfrich refractometers employ only one pass of the light beam through the sample, because multiple passages through the sample are impossible because of the design features of these refractometers.

Turning back the light beam and passing it again through the sample is an unsolvable and complex problem. In order to increase the sensitivity of the refractometer it is possible to use special lenses, which makes the construction of the refractometer very complicated and expensive. Moreover, it will increase the resolution of measurements.

But it is very easy to redirect the light beam in a cell with a cylindrical cell, where the cylinder works as the measuring element and the element that redirects the light beam back into the cell. It is possible many times to repeat measurements and redirect the light beam back to the cylindrical cell.

Refractometer with the testing sample area in the form of a cylinder has a lot of advantages as compared to the refractometers with straight walls (for example, triangle, rectangle, and so on). Besides technical simplicity of the cylinder in a cylindrical cell is much easier to remove the sample after measurements are complete, as compared to the refractometers with straight walls, because it is very difficult to remove the sample from the corners.

The corners of the refractometers are typically gas bubble formation zones, which are usually dissolved in the test samples, and by changing the pressure in the sample liquid; gas bubbles begin to form immediately in the corners of the cell.

Big volume of air bubbles can completely block the work of the refractometer. Even fast pumping of the testing liquid does not always help, as tearing the gas bubble from the corner of the cell is even impossible sometimes. The cylindrical cell's refractometers do not have these problems.

If the outer side of the cylindrical cell is coated by the reflective coating of the light, then the light beams, repeatedly passing through the walls will completely come back in the testing sample [15].

3.2. Influence of the refractive index on the light deviation in the exit of the refractometer

A schematic cross section of the cylindrical cell (cuvette) showing a simplified route of the beam in the measuring system is exhibited in Fig. 3.1. The refractometers measuring system consists of a laser diode, a cylindrical thin-walled cell with its cross section perpendicular to the axis **O** of the cylinder and a linear image sensor. The cell is filled with either immobile or flowing liquid. The position **a** of the beam is identified using a linear CMOS image sensor, the graduated screen with readable divisions being in use for the simplest device design.

The laser beam axis is lined up with the cell's outer wall tangent and is perpendicular to the axis of the cylinder. The laser beam after refraction at point **1** crosses the medium of the cell's wall and arrives at point **2** on the boundary between the material of the cell's inner wall and the liquid. The experiments evidenced that in the vicinity of the critical angle the beams intensity of light is the highest [13].

Therefore, to illustrate the trajectory of the coherent light beam in the cylindrical cell, Fig.3.1 shows only the path of beams that are close to the critical angle, which is equal to the highest intensity on the distribution of intensity of the laser beam. After being refracted at the boundary point **2**, light beams travel through the test liquid and, having crossed it, fall upon the

inner wall of the cylinder at point 3, where they are refracted again and reach the point Q_1 through the medium of the cell's wall.

Because the outside surface of the cylinder is coated with a reflective film the beams falling on this unit area of the boundary surface are reflected and intersect the cell's wall and the liquid several times in a similar way.

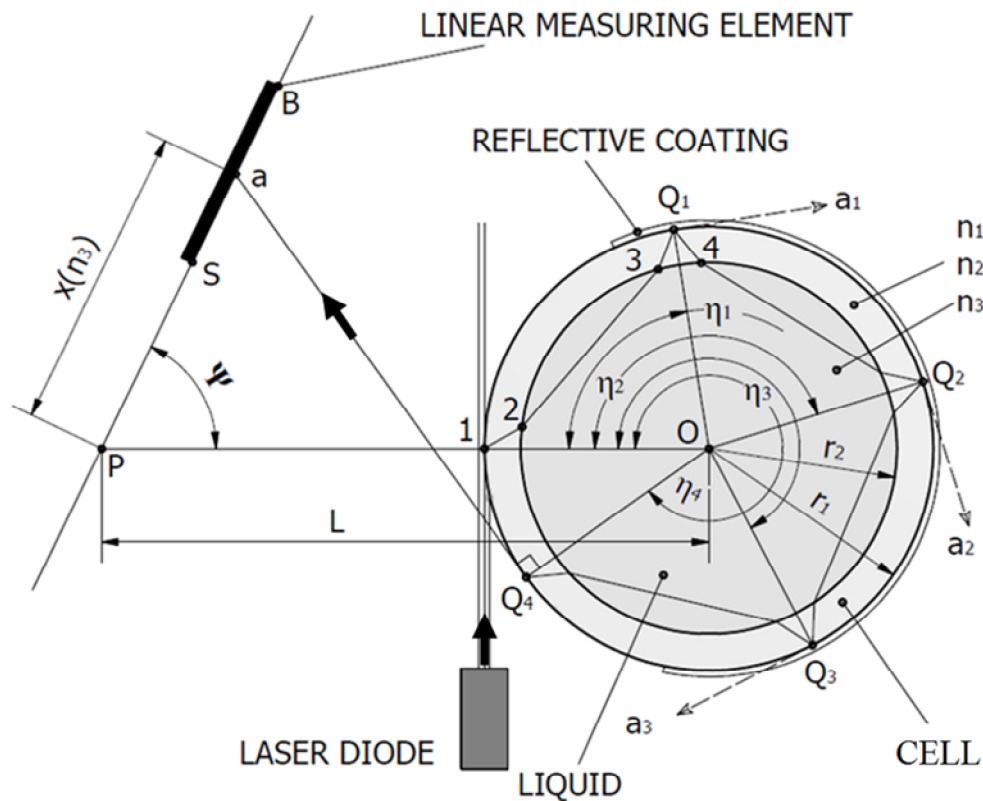


Fig. 3.1. Schematic cross section of the cylindrical cell that illustrates a simplified path of the laser beam in the measuring system

Thereby the light beams hit the outer boundary surface of the cylinder at points Q_1, Q_2, \dots, Q_m (m is the number of consecutive exits of the light beam). If the outer wall of the cell is not coated, Fresnel's equations of light reflection and transmission imply that just a part of the beam gets reflection at each of these points and the rest of the beam is refracted and transmitted into the outer medium as shown in Fig.3.1 with dashed lines a_1, a_2, a_3, \dots .

For a given change in RI, a greater change in the position a of the projection of the exiting beams on the distant linear image sensor is obtained for greater m . Therefore, as an exit with $m \geq 4$ is used, the obtained sensitivity of the measuring system is several times higher than in the case of conventional cell devices [3, 5, 6, 9, 11, 17, 19].

If optical exits Q_m with high m are used for measurements, the light intensity of the exiting beam decreases with each subsequent m . In order to provide light intensity sufficient for accurate detection of the position a , the outer wall of the cell is covered with a reflecting layer, such as vacuum deposited aluminium. The coating covers several or all of the potential beam exits Q_1, Q_2, \dots, Q_{m-1} on the outer wall of the cell prior to the exit Q_m , which is used for taking the measurement. In the example shown in Fig. 3.1, the exit of the beam is created at the point Q_4 on the boundary between the cell's wall and the air.

In addition, the coating of the outside surface also prevents the potential decrease of the intensity of the reflected beams due to condensed moisture or dirt on the outer wall. For this reason, the intensity of the light beam exiting at point Q_m is increased. Accordingly, the reasonable resolving contrast of the beam projection on the linear image sensor is obtained at a higher m [14-15]. Consequently, the limits of the sensitivity and resolution of the refractive index measuring system are extended.

3.3. Cylindrical cell based refractometers and fundamentals of the theory

According to Snell's law Eq. (1.2) (Fig.1.1), we can write for the angles of incident refracted rays at point **1** - α_1 and β_1 , respectively respectively (not shown in Fig.3.1):

$$n_1 \sin \alpha_1 = n_2 \sin \beta_1. \quad (3.1)$$

From here we find

$$\sin \beta_1 = \frac{n_1}{n_2} \sin \alpha_1 \quad (3.2)$$

Since $\alpha_1 = \pi/2$ and RI of air $n_1 \approx 1$, [16, 18]

$$\sin \beta_1 = \frac{1}{n_2}. \quad (3.3)$$

Angle β_1 of the completely refracted ray with respect to the normal of the outside wall of the cylindrical drawn at point **1** expressed as

$$\beta_1 = \beta_{cr} = \arcsin(1/n_2). \quad (3.4)$$

No light is passed to the other medium (e.g., cylindrical glass optical cell) at angles larger than the critical angle β_{cr} .

As the angle of incident ray approaches its limits, $\alpha_1 = \pi/2$, the angle of refracted ray approached its maximum - the critical value β_{cr} .

From Eq. (3.2) it follows that $n_1 = 1$:

$$\beta_1 = \arcsin\left(\frac{\sin \alpha_1}{n_2}\right) \quad (3.5)$$

Derivative of the Eq. (3.5) with respect to α_1 is

$$\frac{\partial \beta_1}{\partial \alpha_1} = \frac{\cos \alpha_1}{n_2 \sqrt{1 - \frac{\sin^2 \alpha_1}{n_2^2}}} \quad (3.6)$$

Under the given circumstances it is possible to use the region around the critical ray for accurate identification of the angle of deflection depending on the RI of the liquid as the ray travels through the optical system of the cylindrical cell. As this critical ray arrives at point **2**, we may write a relation between the angle of incidence α_2 and the angle of refraction β_2 similar to that at point **1**:

$$n_2 \sin \alpha_2 = n_3 \sin \beta_2, \quad (3.7)$$

wherefore it follows that

$$\beta_2 = \arcsin\left(\frac{n_2}{n_3} \sin \alpha_2\right), \quad (3.9)$$

hold for the ray refracted at point **2**. At a certain value of RI n_2 of the optical cell material and sufficiently small inner radius $r_{2\min}$ it is possible that a ray refracted at point **1** does not cross the inner wall of the cylinder.

The critical radius of the inner wall is:

$$r_{2\min} = r_1 / \sin \beta_1. \quad (3.10)$$

With account for (2.1), $r_{2\min} = r_1 / n_2$, and $r_1 / r_{2\min} = n_2$.

From Eq. (3.5) the ratio

$$k = r_1 / r_2, \quad (3.11)$$

must satisfy the inequality:

$$k < n_2. \quad (3.12)$$

A ray refracted at point **2** passes through the liquid and arrives at a point on the inner surface of the cylindrical cell under condition that

$$n_3 < n_2 \quad (3.13)$$

It is very important to take into consideration these formulas (2.10), (2.12) and (2.13) when choosing the size of the projected measuring cell of the refractometer!

This condition puts limits to the smallest measurable value of the RI. A ray is refracted at point **3**, travels through the cell wall and reaches the outer wall at point Q_1 .

The analytical calculation of the RI of liquids contained in the system described above is provided by applying the laws of light refraction and reflection and using a simple trigonometric formulae, the central angle η_m (see Fig. 3.1 for the case when $m = 4$) was calculated as:

$$\eta_m = 2m[(\pi/2 - \arcsin(k/n_3) + \arcsin(k/n_2) - \arcsin(1/n_2) + \alpha)], \quad \text{rad}, \quad (3.15)$$

where $k = r_1/r_2$ is the ratio between the outer and inner radii of the cylindrical cell; n_2 and n_3 are the refractive indices of the material of the cell and the liquid, respectively; α - central angle of the laser impact position in the tangential line on the lateral surface of the cell.

The angle α must be taken into account in Eq.(3.15) for adjusting the laser beam entering the sensitive surface of the linear optical element, to cover the whole measuring range of the refractometer. If the laser beam enters the sensitive area of the linear optical element, it is necessary to provide the deviation of the angle in a clockwise direction, the sign is positive; when the deviation of the angle is contraclockwise, this sign is negative. See Fig. 3.2.

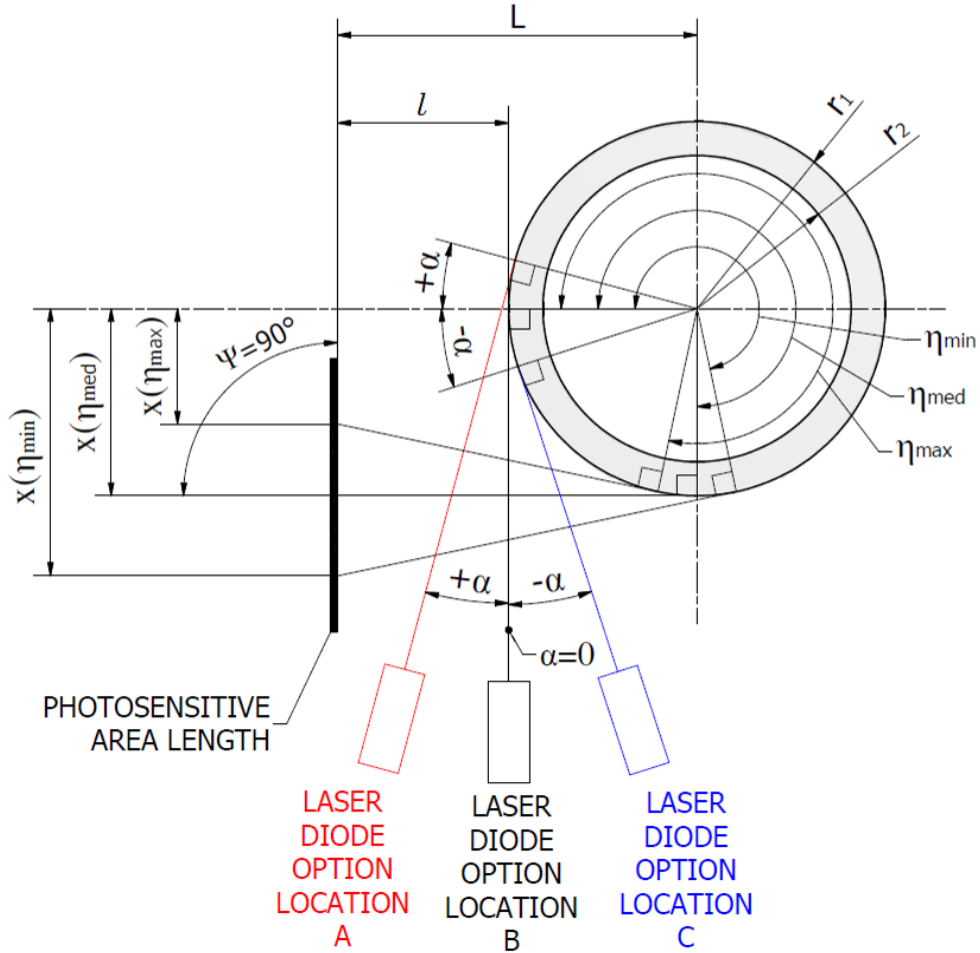


Fig. 3.2. α - central angle of the laser impact position in the tangential line on the lateral surface of the cell

The measuring sensitivity is characterized by the derivative of the function (3.15) with respect to the refractive index of the liquid, (n_3):

$$d\eta_m / dn_3 = 2mk / [(n_3)^2 (1 - k^2 / (n_3)^2)^{1/2}]. \quad (3.16)$$

It is shown in Eq.(3.16) that the projection's position \mathbf{a} on the linear image sensor for the beam outgoing from the exit Q_4 in respect to n_3 , optical and geometrical parameters of the cell and the parameters of the measuring system ψ and L , can be calculated as:

$$x(n_3) = \frac{L \cos \eta_4 - r_1}{\cos(\eta_4 + \psi)}, \text{ (mm)}, \quad (3.17)$$

Dependence of angle η_m on the refractive index of the liquids n_3 with respect to the choice of exit points Q_1 , Q_2 , Q_3 and Q_4 , i.e., value of m ($m = 1, 2, \dots, 4$), according to Eq.(3.15) is illustrated in Fig.3.3.

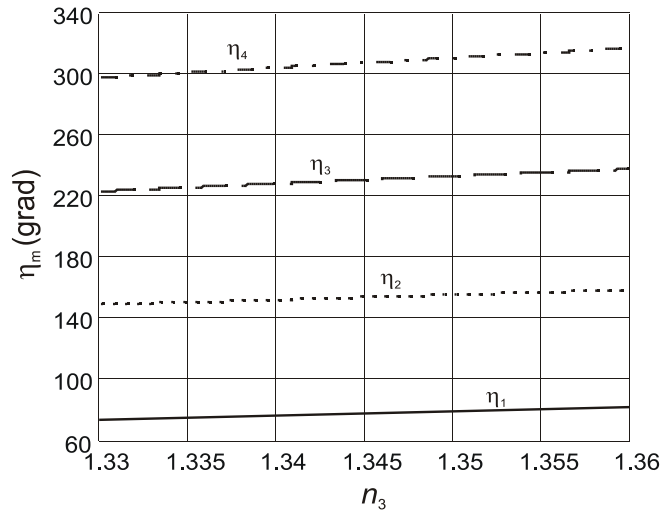


Fig. 3.3 Angular positions η_1, η_2, η_3 and η_4 , of the respective output points Q_1, Q_2, Q_3 and Q_4 as functions of refractive index n_3

Each subsequent reflection of the laser beam (inside in the cell) significantly increases the sensitivity of the refractometer. If at the point Q_1 have barely noticeable inclination characterizing the movement of the central angle n_1 , than at the point Q_4 the central angle η_4 has a very significant slope that shows how much increases the sensitivity of the refractometer.

Analysis of Eq.(3.16) shows that the multiple angular sensitivity of the outlet point $\partial\eta_4/\partial n_3$ and, consequently, the equal growth in sensitivity of the refractometer can be achieved by optimising the ratio of outer and inner radii $k = r_1/r_2$, that is, the wall thickness of the cylindrical cell.

An illustration of that at $\eta_m = \eta_4$, ($m=4$) is shown by $\partial\eta_4/\partial n_3(n_3)$ diagrams in Fig. 3.4.

These diagrams are crucial because they demonstrate the importance of determining the ratio of the outer and inner radius of the cell. For very thin cell walls ($k = 1,15$) we have a little gradient, and when the walls are thick ($k = 1,30$) we have a very big gradient that is not linear. The optimum would be $k = 1,25$.

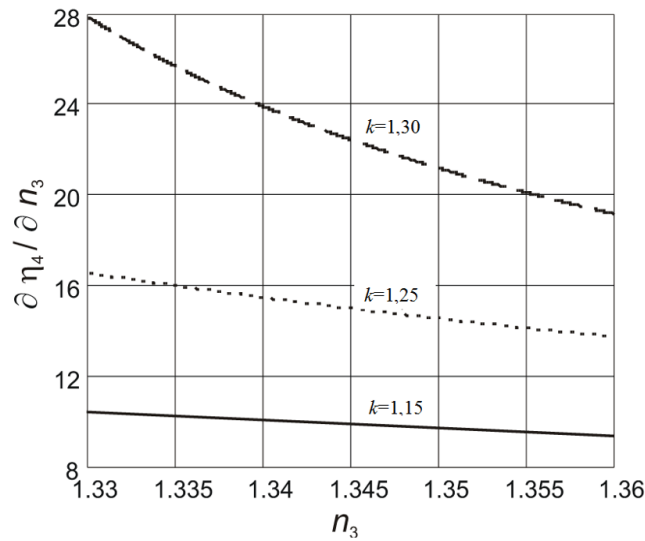


Fig. 3.4. Angular sensitivity $\partial\eta_4/\partial n_3$ of output beam of the optical cell as function of refractive index n_3 at different outer-to-inner radius ratios $k = r_1/r_2$

By using Eq.(3.15) and Eq.(3.17) and maintaining the notation used earlier, the function $x(n_3)$ can be expressed as:

$$x(n_3) = \frac{L \cdot \cos \left[2m \left(\frac{\pi}{2} - \arcsin \left(\frac{k}{n_3} \right) + \arcsin \left(\frac{k}{n_2} \right) - \arcsin \left(\frac{1}{n_2} \right) \right) + \alpha \right] - r_1}{\Delta p \cdot \cos \left[\psi + \left[2m \left(\frac{\pi}{2} - \arcsin \left(\frac{k}{n_3} \right) + \arcsin \left(\frac{k}{n_2} \right) - \arcsin \left(\frac{1}{n_2} \right) + \alpha \right) \right] \right]} , \quad (3.18)$$

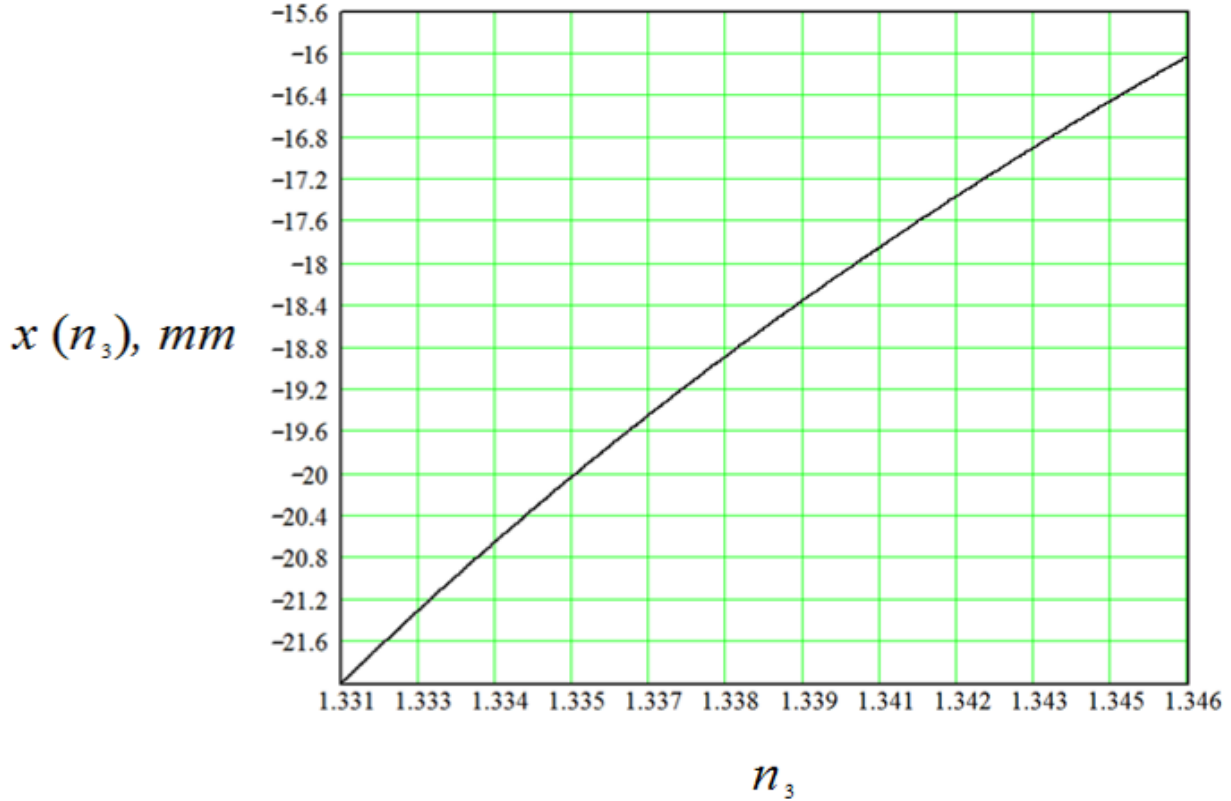


Fig.3.5. The calculated position of the exiting laser beam projection on the CMOS linear image sensor, as a function of the refractive index of the liquid contained in the cell

In addition to the notation used previously, we introduce the sensor position parameter $x(n_3)$, equal to the distance between the point \mathbf{P} and the coordinate \mathbf{a} of the linear measuring sensor on the line \mathbf{Pa} (see Fig.3.1). Therefore, it is possible to assign the sequential number 1 to the initial pixel of the linear image sensor.

Therefore, it is possible to assign the sequential number 1 to the initial pixel of the linear image sensor. By using Eq.(3.15) and Eq.(3.17) and maintaining the notation used earlier, for CMOS linear image sensor, if known pixel dimensions Δp , you can determine the number of pixels on the move - $p(n_3)$.

$$p(n_3) = \frac{x(n_3)}{\Delta p}, \quad (3.19)$$

Theoretical the resolution of the measurements of the future refractometer can be calculated using the formulas Eq.(3.19).

$$\delta = \frac{n_{3T1} - n_{3T2}}{p(n_{3T1}) - p(n_{3T2})} = \frac{n_{3T1} - n_{3T2}}{\Delta p}, \quad (3.20)$$

where:

n_{3T_1} - the refractive index of the liquid where the temperature t_1 is taken from the reference literature,

n_{3T_2} - the refractive index of the liquid where the temperature t_2 is taken from the reference literature,

$$\Delta p = p(n_{3T_1}) - p(n_{3T_2})$$

Formulas Eq.(3.15), Eq.(3.18), Eq.(3.19), Eq.(3.20) are basic and sufficient in mathematical modelling and are suitable for all cases of the new design of the cylindrical cell based refractometer.

Using Eq. (3.15), Eq. (3.18), Eq. (3.19), Eq. (3.20) in the thesis a mathematical simulation of some multiple design options of refractometers is made.

Table 3.1 shows the approximate input data of physical and geometrical parameters of the simulated refractometers and expected parameters of these parameters.

3.4. Mathematical simulation of the refractometers

By using Eq.(3.15), Eq.(3.18), Eq.(3.19), Eq.(3.20) It is possible to completely preliminary calculate all the basic parameters of the newly designed refractometers.

We can mathematically simulate several types of the refractometers, and then in the 4th chapter of this work we will give a comparison of the calculated parameters with the real experimental data (for some of these new types).

Table 3.1

Initially stated and expected parameters of the refractometers

Parameters	The simplest refractometers	Refractometer A	Refractometer B	Refractometer Fig.3.6.
λ, nm	635	635	635	635
r_1, mm	5.1	5.5	5.5	5.98
r_2, mm	4.5	4.5	4.5	4.5
n_2	1.515	1.515	1.515	2.185
L, mm	117.1	10.5	10.5	10.98
l, mm	112	5	5	5
α	-46.6°	-28.6°	-68°	+6°
Ψ	90°	90°	90°	90°
m	4	4	4	22
$\Delta p, \mu m$	Scale 35.6 mm	7.8	7.8	1.12
Temperature compensation	No	Yes	Yes	Yes
RI	1.3312...1.3651	1.33167...1.36454	1.33167...1.34583	1.3318...1.3324
δ, RI	10^{-3}	5.7×10^{-5}	2×10^{-5}	2×10^{-7}

If window into the evaporated surface of the cell is sufficient only to enter the laser beam and when we have a large number of multipath reflections m inside the cell, we let the beam go spiral, as shown in Fig.3.6. **Then, the number m theoretically may be multiple, and it is possible to have nearly infinite sensitivity of the refractometer.**

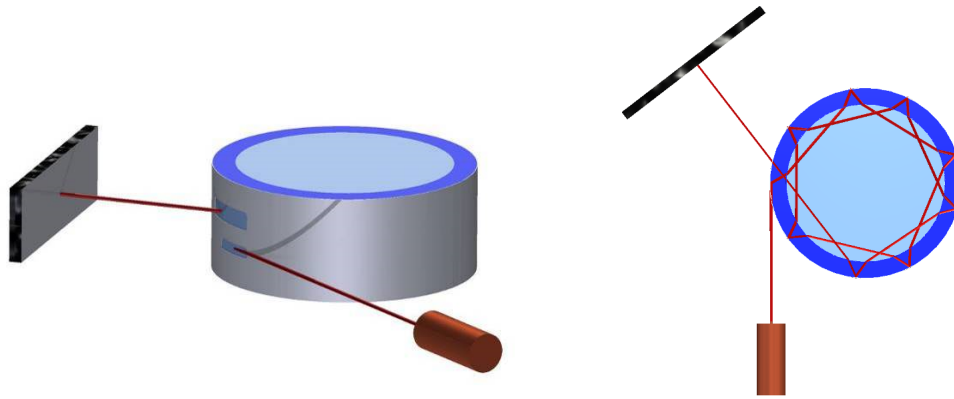


Fig.3.6. The laser beam go spiral

3.5. Approach to analyse the image by cylindrical cell based refractometer

Projected on a linear measuring element (for example, on a CMOS linear image sensor), the beam forms an image area containing a *front*, namely, a transition region from darkness to light (as shown in Fig. 3.7.). The position of the front is determined by the critical angle of the optical system comprising the cell and the liquid being measured. Usually this front is used to define and detect the projection position of the beam passed through the cylindrical cell [14, 15].

Since the transition between the dark and light parts of the image is gradual, it is necessary to define the position of the boundary. This position is usually defined as the point where the light intensity distribution graph is the steepest and is calculated for each RI value, an ordinal number of a pixel (a position) on the image sensor is thus assigned.

Such an approach, however, has some disadvantages. The distribution of the light intensity on the front depends on the slope of the light intensity graph, the intensity and stability of the light source and the presence of some colloidal particles or small gaseous bubbles in the measured liquid. Consequently, the detection of the front position is indeterminate and sometimes even impossible, particularly in the case of flowing liquids.

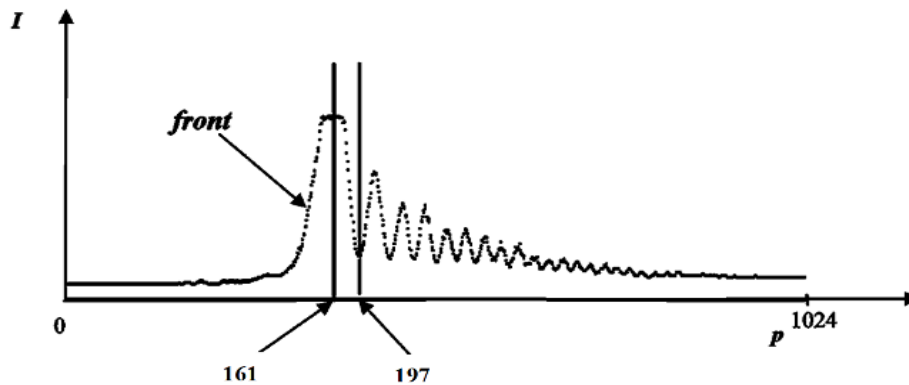


Fig. 3.7. Overall image on a linear optical sensor p =number of pixels (Hamamatsu CMOS monochromatic linear 1024 pixel image sensor S9226), I - intensity of the light

The Fig. 3.8 (only the part of the images Fig. 3.7 is shown) presents diagrams of the beam for image position detection due to the developed [14, 15] and conventional techniques [2, 3, 5, 6, 8, 9, 11, 17, 19], the cell contains the distilled water. The solid vertical lines shown in Fig.3.8. represent the positions detected by the developed technique, while the dashed vertical lines correspond to the positions determined by the conventional technique.

Another method for determining the position of the illuminated area of the light beam projection on the linear image sensor has been developed in to increase the resolution and the

resolution of the measuring device and to practically eliminate the bulk of the effects caused by the varying intensity of the light source and the influence of gas bubbles or admixtures of particles on the quality of measurements. This method is based on the detection of the location of the beam projection image, which is fixed by Eq.(3.17). The whole width of the image is several tenths of a millimetre. A narrow area of each entire image is scanned by the sensor and characterizes the light intensity distribution of the cross section of projected beam over the area of the sensor. Waveform of the images shows that the interference of laser light after it is reflected from different regions in the cell generates an interference pattern, as described in more detail in [14, 15].

The image position is determined by the position of the first or any subsequent minimum following the position of the maximum intensity of distribution. From the whole image of the beam projected on the linear sensor, the location of the minimum intensity is used as a conveniently and precisely detectable position.

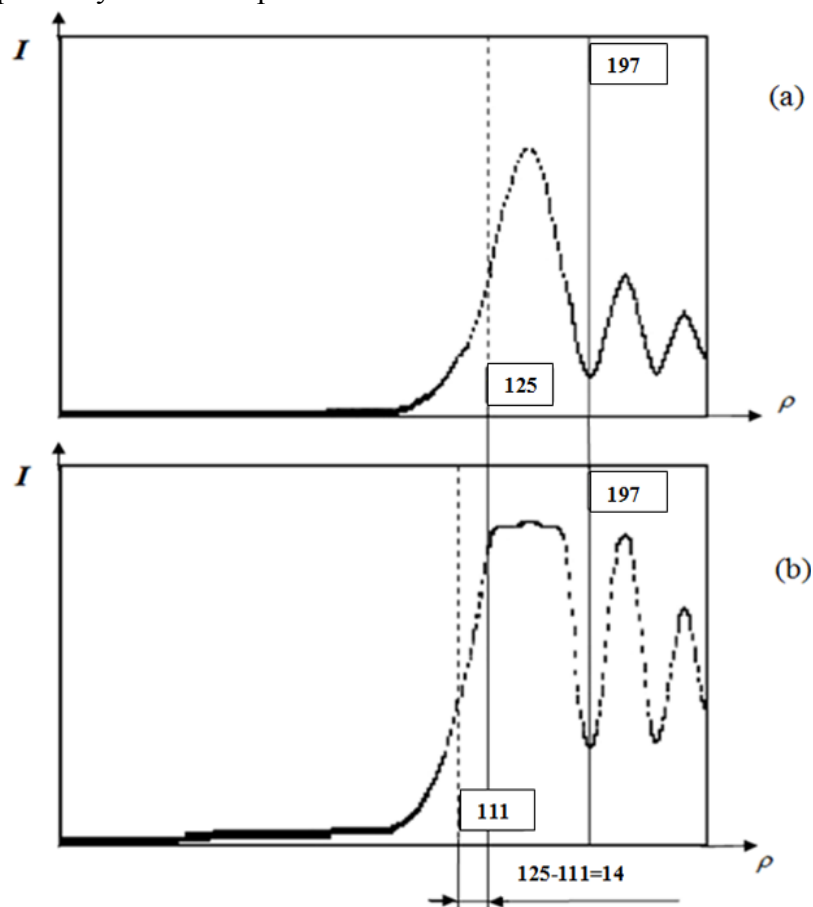


Fig.3.8. Detection of the position of the image at two different light intensities of the laser beam projection on the linear image sensor
 I – intensity of the laser beam; p – number of pixels

Chapter 4. CYLINDRICAL CELL BASED REFRACTOMETERS FOR MEASUREMENTS OF REFRACTIVE INDEXES OF LIQUIDS

In this chapter the following tasks are described:

- elaboration of CCR prototypes, description of the stand for studies of the physical parameters for the CCR,
- the RI and concentrations of solutions measuring methodologies by new CCR and the calibration methodology,
- investigation of the physical parameters for the prototype.

4.1. Scheme of the refractometers

For the purpose to maintain the experimental integrity, e.g., to use a common cylindrical cell, laser and a linear optical element, as well as to reduce the cost of the experiment, the new design of the refractometer has been developed, in which both options A and B was implemented in the single constructive device.

On Fig.4.1 shows the optical block of the precision electronic unit cells refractometer.

From a laser diode pos.4 a laser beam pos.3 passes a collimator pos.5 (which is made as a simple aperture) and enters in the cell pos.8, passes inside the cell (Fig.3.1) and after passes out of the cell pos.7, and falls on a photosensitive surface a Hamamatsu CMOS where a monochromatic linear image sensor S9226 pos.2.

Since the distance from the laser diode is less than 8 mm, it was experimentally determined that collimator device pos.5 may be formed as a simple aperture with a gap of 1 mm. The aperture is parallel to the central axis of the cell. The wavelength of the laser diode is 635 nm, the power is 5 mW.

As we can see on Fig.4.1, we can invert PCB (pos. 1) upside down, and by changing the inclination angle of the laser α we can obtain the version A and version B.

Fig. 4.2 shows one of the developed RI measurement devices.

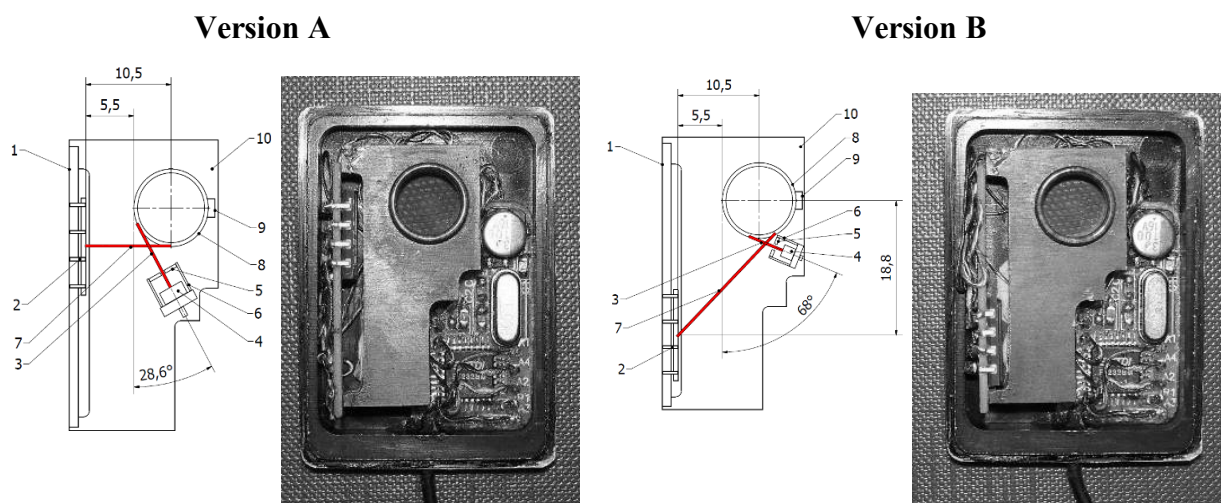


Fig.4.1 Schemes of the optical systems of precision refractometers and inside views for versions A and B



Fig.4.2. The device is used for the experimental tests mentioned in the note (dimensions 49 mm x 35 mm x 8 mm)

4.2. Algorithm of processing of measurements results

Fig. 4.3 and Fig. 4.4 show an algorithm for measuring the concentration of the solution and the RI. This algorithm consists of two parts: sensor unit (A) and the information processing unit and the display unit (B). When you turn on the device, in the block (A), the minimum of the laser beam intensity $I = 0$ is settled and the counter of the pixel numbers is reset to $p = 0$.

After the laser impulse, begins the reading process of the accumulated charges $U(p)$ from each of the 1024 pixels of the linear optical element by using microcontroller (MCU internal ADC). In the block (A), data $U(p)$ for each pixel of the sensor does not accumulate, they are immediately transmitted to the remote device through USART or USB (computers, mobile phones, tablets, or to some specialized remote units with visual indication) – the block (B).

At the same time is looking for the maximum value $U(p)$, this is compared with the threshold $U_{threshold}$ and the intensity of the laser beam I is adjusted, regulating the laser pulse duration on the sensitive surface of the sensor. This is necessary to obtain a high-quality graphics of the intensity distribution of the laser beam on the sensor pixels, when determining the number of pixel p_m of the first minimum in the chart.

In the algorithm the temperature T parameters from the cell with the test solution are acquired and they are immediately transmitted via USART or USB to the remote device—the block (B).

The algorithm of the block (B) provides the procedure of work of the remote device. Here, the data $U(p)$ are collected in the data array $M(p)$. Further, from the array of $M(p)$ the number of pixel p_m for the first minimum in the plot of the intensity distribution of the laser beam is determined. According to the number of the first minimum pixel p_m and data of the temperature T , by using the mathematical formulas (from Eq.(4.1) to Eq.(4.5)) RI and the concentration of the test solution are detected. The calculated data are displayed on the display.

By combining two algorithm blocks (A) and (B) in one block, without remote USART or USB communication, we can obtain a compact hand-held, self-powered refractometer.

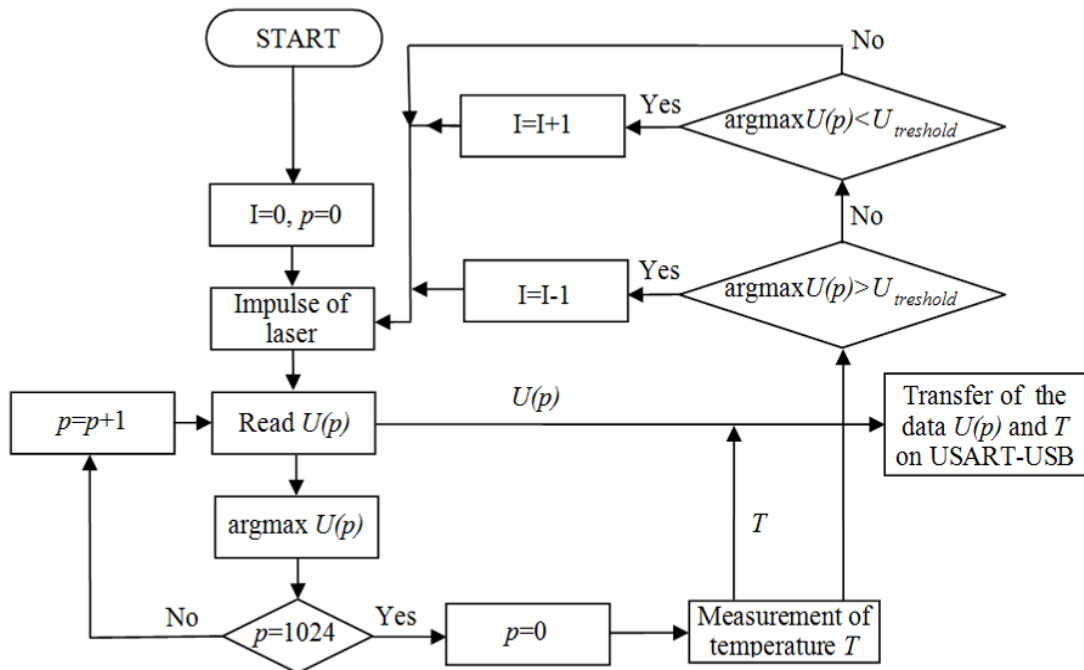


Fig. 4.3. Algorithm for solutions concentrations and RI measurements, sensor block (A)

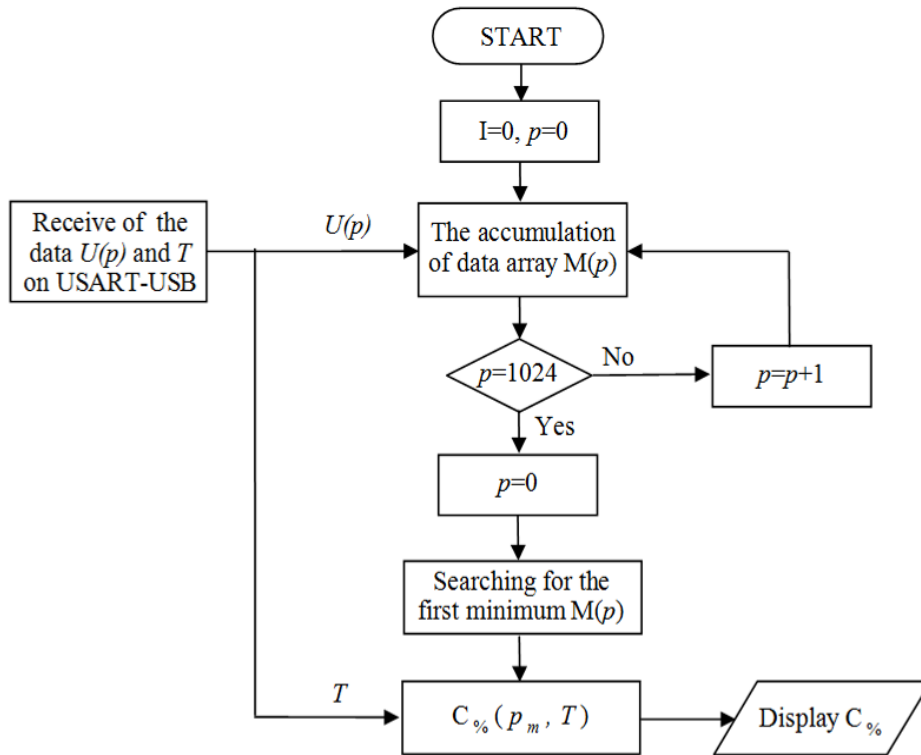


Fig.4.4. Algorithm for solutions concentrations and RI measurements, information processing and the display block (B)

4.3. The calibration of the refractometers

To verify the derived formulas Eq. (3.15), Eq. (3.18), Eq. (3.19), Eq. (3.20) and the results of mathematical modelling the simplest refractometer, the refractometer with a large RI measuring range, the accurate refractometers with a small RI measuring range (see Table 3.1) have been made and calibrated with the ethanol, NaCl and sucrose aqueous solutions. Also has been made the special technological stand for testing and calibration.

The solutions have been prepared by using a precision hydrometer (for calibration of ethanol aqueous solutions) and precision weighing instrument (for calibration of NaCl and sucrose aqueous solutions), at standard temperature of 20°C (concentration -% weight/vol.). Refractometer has been placed in a specially made thermostat with the temperature setting of $\pm 0.1^\circ\text{C}$.

For the temperature measurements a platinum thermal sensor (resolution $\pm 0.02^\circ\text{C}$) was in use. The mathematical computation of the temperature-compensated ($c_{\%TC}$) concentration (% weight/vol.) of a given liquid sample is based upon a polynomial calibration equation (obtained as shown below). In order to illustrate the proposed computations, an example for thermo-compensated measuring device was provided (see below an example of calibration of the refractometer with a large RI measuring range for ethanol aqueous solution).

Calculation of the thermo-compensated volume concentration of a binary liquid sample was carried as follows:

- By splitting of the measurement range of sample concentration into smaller. The range from 0% to 70% weight/vol.
- By preparation and arranging of the measured data p_s (Table 4.1) by ascending percentages of concentration. Recording of the measured concentration of the reference sample $c_{\%R}$ (number of pixels) p_s at the measured temperatures t_f 15°C, 20°C and 25°C.

Table 4.1

Measured p_s values according to the reference sample concentration $c_{\%R}$ and the measured sample temperatures t_f , by using refractometer A

Ethanol concentration, $c_{\%R}$	Temperature, t_f	p_s
0 %	15°C	220
	20°C	208
	25°C	196
2.5 %	15°C	249
	20°C	238
	25°C	226
5 %	15°C	283
	20°C	272
	25°C	260
7.5 %	15°C	319
	20°C	308
	25°C	298
10 %	15°C	355
	20°C	345
	25°C	334
20 %	15°C	497
	20°C	487
	25°C	478
30 %	15°C	610
	20°C	601
	25°C	592
40 %	15°C	690
	20°C	682
	25°C	673
50 %	15°C	743
	20°C	734
	25°C	726
60 %	15°C	776
	20°C	768
	25°C	759
70 %	15°C	797
	20°C	789
	25°C	781

- Using the p_s values (measured at the sample temperature of 15°C) to perform a regression analysis. Similarly, using the appropriate values at the sample temperatures of 20°C and 25°C the calibration equations were obtained.
- Refractometer was designed as a multi-purpose device, it was necessary to provide the calibration process by taking into account the 3rd order polynomials [18]. When using a non-linear mathematical regression analysis, ethanol volume percentage concentration (c%), depending on the calibration equation p values were calculated as follows:

$$C_{\%15} = -51.39972 + 0.36626 \cdot p - 7.53542 \cdot 10^{-4} \cdot p^2 + 6.03566 \cdot 10^{-7} \cdot p^3 \quad (t=15^\circ\text{C}), \quad (4.1)$$

$$C_{\%20} = -43.23919 + 0.31635 \cdot p - 6.51164 \cdot 10^{-4} \cdot p^2 + 5.39917 \cdot 10^{-7} \cdot p^3 \quad (t=20^\circ\text{C}), \quad (4.2)$$

$$C_{\%25} = -41.97363 + 0.32174 \cdot p - 6.8533 \cdot 10^{-4} \cdot p^2 + 5.79868 \cdot 10^{-7} \cdot p^3 \quad (t=25^\circ\text{C}), \quad (4.3)$$

The quadratic values of the correlation coefficients curves corresponding to equations (4.1), (4.2), (4.3) are $R^2=0.99676$, $R^2=0.99839$, $R^2=0.99687$.

Because p – the linear optical element number can vary from 1 to 1024, its raising to the 3rd power can obtain a significant value, therefore the third-order polynomial can not be ignored.

Calculation of the thermo-compensated volume concentration $C_{\%TC}$

For $+15^\circ\text{C} < t_m < 20^\circ\text{C}$:

$$C_{\%TC} = C_{\%15} + [(C_{\%15} - C_{\%20}) (20 - t_m)] / \Delta t, \quad (4.4)$$

where $\Delta t = 20 - 15 = 5$.

For $+20^\circ\text{C} < t_m < 25^\circ\text{C}$:

$$C_{\%TC} = C_{\%20} + [(C_{\%20} - C_{\%25}) (25 - t_m)] / \Delta t, \quad (4.5)$$

where $\Delta t = 25 - 20 = 5$.

Doing exemplary calculation of the thermo-compensated volume concentration $C_{\%TC}$ of a given ethanol-water mixture sample:

a) For the actual sample temperature t_m and concentration p (expressed in notional units p) measured and fixed using the developed measuring device.

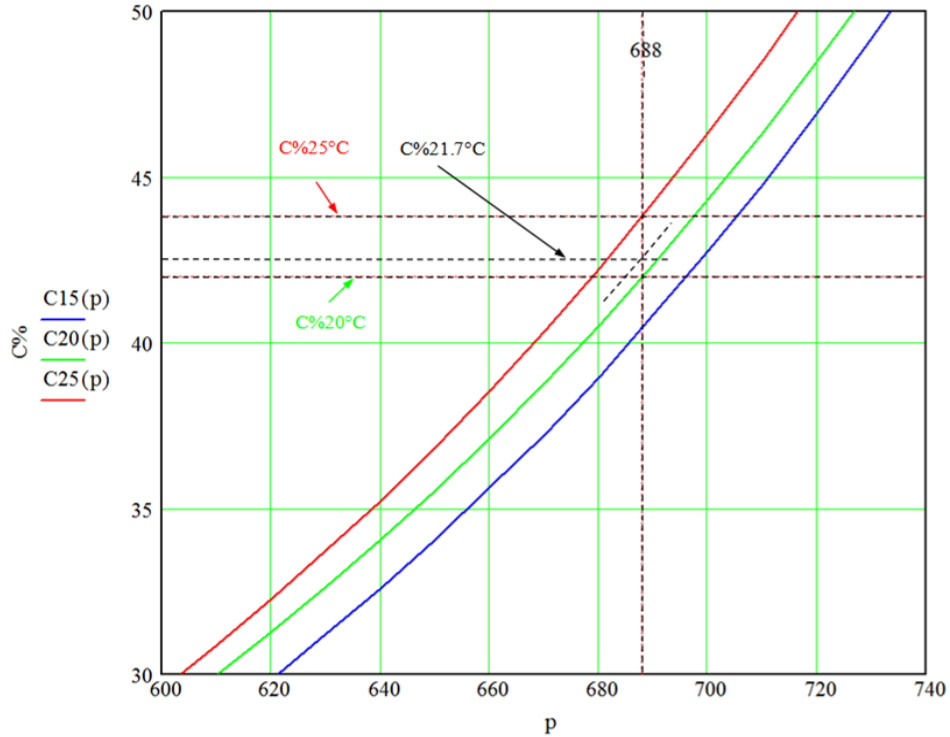


Fig. 4.5. The calculated thermo-compensated weight concentration $C_{\%}$ for a given ethanol-water mixture sample at the actual measured sample temperature t_m (p -number of pixels)

For the chosen sample the values $t_m = 21.7^\circ\text{C}$ and $p = 688$ are measured and recorded.

b) Using Eq.(4.2) and Eq.(4.3) and assuming $p = 688$, the following volume percentages are obtained:

$$C_{\%20} = 42.015\%, \text{ and } C_{\%25} = 43.827\%$$

c) Substituting the above $C_{\%}$ values, for $t_m = 21.7^\circ\text{C}$ the thermo-compensated liquid measured concentration is calculated by the Eq.(4.5), as a result, will have: $C_{\%TC} = 42.631\%$

The microcontroller of the sensor unit performs the calibration and recording of measured data as well as processes the data of the previous example, and records the final results.

Table 4.2

Measured p_s values according to the reference sample concentration $c_{\%R}$ and the measured sample temperatures t_f , by using refractometer B

Ethanol concentration, $c_{\%R}$	Temperature, t_f	p_s
0 %	15°C	230
	20°C	197
	25°C	164
5 %	15°C	397
	20°C	368
	25°C	339
10 %	15°C	578
	20°C	552
	25°C	526
15 %	15°C	747
	20°C	724
	25°C	701
20 %	15°C	895
	20°C	874
	25°C	854

4.4. Approach to properties of the refractometers

To determine the resolution of RI for each refractometer option, it is necessary to use Eq. (3.20).

For the refractometer with a large RI measuring range (refractometer A) for ethanol aqueous solutions, accordingly, at $t_1 = +15^\circ\text{C}$, $n_1 = 1.33264$, and at $t_2 = 25^\circ\text{C}$, $n_2 = 1.33158$ [4, 7]. Measurements show that the first minimum of the optical intensity distribution changes its position from pixel $p_1 = 220$ at $t_1 = +15^\circ\text{C}$ to pixel $p_2 = 196$ at $t_2 = +25^\circ\text{C}$.

In accordance with the given parameters of the optical system, the resolution of the measuring device $\delta = \delta n / \delta p$ (where $\delta n = |n_1 - n_2|$ is the difference in refractive indices, $\delta p = |p_1 - p_2|$ the difference in detected positions) before mathematical processing of the data is about $\delta = 5.6 \cdot 10^{-5}$ RI per pixel.

Analogue, for the accurate refractometer with a small RI measuring range (refractometer B): $t_1 = +15^\circ\text{C}$, $n_1 = 1.33247$, and at $t_2 = 25^\circ\text{C}$, $n_2 = 1.33113$ [4, 7], $p_1 = 230$ at $t_1 = +15^\circ\text{C}$ to pixel $p_2 = 164$ at $t_2 = +25^\circ\text{C}$ when we substitute in Eq.(3.20), we will obtain $\delta \approx 2 \cdot 10^{-5}$ RI per pixel.

Similarly it is possible to obtain the resolution per pixel for concentrations of ethanol, NaCl and sucrose aqueous solutions (see Table 4.3).

Table 4.3

Initially stated and expected parameters of the refractometers

Parameters	Refractometer A	Refractometer B
RI	1.33167..1.36454	1.33167..1.34583
Ethanol, $\delta_{simulation}$, RI	5.7×10^{-5}	2×10^{-5}
Ethanol, δ_{real} , RI	5.6×10^{-5}	2×10^{-5}
Ethanol, % weight/vol	0-70	0-20
$\delta_{ethanol}$, % weight/vol.	0.12	0.03
NaCl, % weight/vol	0-25	0-9
δ_{NaCl} , % weight/vol	0.032	0.012
Sucrose, % weight/vol	0-25	0-10
$\delta_{sucrose}$, % weight/vol	0.036	0.014

In order to test the resolution of this measuring system, two images were detected on the linear measuring sensor at two different light intensities of the beam exiting the cylindrical cell. Distilled water in the cylindrical cell was maintained at a temperature of $+20^{\circ}\text{C} \pm 0.02^{\circ}\text{C}$. Fig.3.8.

The accurate refractometer option with a small RI measuring range has been used (see Table 4.1. Refractometer B).

The images shown in Fig.3.8(a) at the nominal light intensity I_1 of the exiting beam (in relative units), while demonstrates the distribution of the optical intensity of the incident beam over the area of the linear image sensor.

The position of the image is detected using the position of the first minimum of the waveform light intensity distribution over the image sensor, which in this case corresponds to the pixel number 197 marked by the solid vertical line shown in Fig.3.8(a). The dashed line marks the pixel's position 125 residing on the steepest part of the light intensity distribution at the boundary between illuminated and dark transition regions, and corresponds to another method of image detection [14, 15].

Figures Fig.3.8(b) illustrate the case when the laser intensity was increased 2.5 times and show the light intensity distribution over the linear sensor. It follows from Fig.3.8(a) and Fig.3.8 (b) that such a change of measuring conditions has no effect on the image position marked by the pixel number 197.

The conventional method of image detection [2, 8, 16, 18] under the same conditions leads to the image position shift by $125-111=14$ pixels.

Considering the resolution of the device mentioned above and used in the measurement $\delta \approx 2 \cdot 10^{-5}$ experimentally determined with no mathematical processing and averaging, a deviation of $\delta \times 14$ pixels leads to a measurement error of $2.8 \cdot 10^{-4}$ RI.

CONCLUSIONS

1. The basic operating principles for CCR were developed, where an optical beam refraction and multiple reflections in a cylindrical cell are used; thereby increasing the RI measurement resolution by one power and achieving $MR = 10^{-5}$.
2. The mathematical model has been developed and analyzed, which takes into account the temperature effect on the detection of resolution, the possibility to achieve the resolution up to 10^{-7} has been demonstrated. It has been shown; that the multiple light beam passage through cylindrical cell with test liquid increases the RI measurement resolution in line with the number of the passage cycles.
3. The RI measurement algorithm and measurement method have been developed, where a minimum place of the detectable beam interference pattern has been used, that allows to achieve the RI measurement resolution $2 \cdot 10^{-5}$. The calibration and verification of CCR prototypes for ethanol, NaCl and sucrose aqueous solutions have been provided. The RI measurements (with the resolution of $2 \cdot 10^{-5}$) for all the above mentioned solutions have been achieved. The applicability of CCR to identify concentrations of ethanol, NaCl and sucrose were tested. The corresponding resolutions of the following weight/vol. were achieved: 0.03%; 0.012%; 0.014%.
4. CCR prototypes have been designed and developed (including optical, electronic, computing and mechanical systems) to verify practical applications-possibilities of the refractometers.
5. CCR were implemented for practical use at 8 research and industrial institutions (3 in Latvia, 2 in Germany, 3 in USA).

REFERENCES

1. Harvey A. H., Gallagher J. S. and Levelt Sengers J. M. H. Revised formulation for the refractive index of water and steam as a function of wavelength, temperature and density // *J. Phys. Chem. Ref.* -1998, - 27, -773.
2. *Instruction Manual for In-line Refractometer PR-03*, -2000, -p.123.
3. Krishna V., Fan C. H. and Longtin J. P. Real-time precision concentration measurement for flowing liquid solutions // *Rev.Sci. Instrum.* -2000, <http://dx.doi.org/10.1063/1.1288236>.
4. Lide R., (ed.) *CRC Handbook of Chemistry and Physics // Internet Version 2005*, <<http://www.hbcpnetbase.com>>, CRC Press, Boca Raton, FL, 2005.
5. Longtin J. P. and Fan C. H. Precision laser-based concentration and refractive index measurement of liquids// *Microscale Thermophys. Eng.* -1998, -pp.261–272.
6. Narayanan V. A., Narayanan R. Laser-based liquid prism sucrosemeter - a precision optical method to find sugar concentration. // *J. Chem. Educ.*, 1997, 74 (2), p 221.
7. *Refractive index database. Optical constants of 1000+ materials./Internets.-
<http://www.refractiveindex.info/>*
8. Salo H. *Refractometer // US Patent No 6,067,151.*, -2000.
9. Samedov F. Laser-based optical facility for determination of refractive index of liquids // *Optics and Laser Technology.*, -2006,- 38, - pp.28–36.
10. Sorensen H. S., Pranov H., Larsen N. B., Bornhop D. J. and Andersen P. E. 2003 Absolute refractive index determination by microinterferometric backscatter detection // *Anal. Chem.*, -2003., -75(8), -pp.1946–1953.
11. Synovec R. E. Refractive index effects in cylindrical detector cell designs for microbore high-performance liquid chromatography// *Anal. Chem.*-1987, -59(24), -pp.2877–2884.
12. Vilitis O., Kozlovs V., Merkulovs D., Plaša diapazona šķidrumu laušanas koeficienta mērīšanas paņēmieni un refraktometrus tā īstenošanai. // *Patents LV13294, International Publication Date 20.05.2005.*
13. Vilitis O., Merkulovs D., *Optical cell for measuring refractive index and concentration of liquids. // Latvian Journal of Physics and Technical Sciences, Riga, 2004, 4 p.58–66.*
14. Vilitis O., Merkulovs D., *Refraktometra gaismas staru kūļa optiskā attēla detektēšanas paņēmieni // Patents LV13598, International Publication Date 20.09.2007.*
15. Vilitis O., Šipkovs P., Merkulovs D., *Šķīdumu koncentrācijas mērīšanas paņēmieni un sensors tā īstenošanai // Patents LV13728, International Publication Date 20.07.2008.*
16. Wolf K.B. (1995), *Geometry and dynamics in refracting systems, European Journal of Physics.*, =1995., -16, -pp.14–20.
17. Горшков А.И., Ошуркова О.В., Константинов В.Б. Повышение чувствительности рефракционного метода регистрации на границе в капиллярных методах разделения // *Журн. техн. физ.* -2001, -71(5), -119–122.
18. Иоффе Б.В. *Рефрактометрические методы химии.* - Ленинград: Химия, 1983, 352с.
19. Чернов С.М., Жилик К.К., Рабзонов П.Г. Определение показателя преломления жидкостей и газов в капиллярах // *Журн. приклад. спектр.* -1982, -37, -455–459.